

# On the toroidal-velocity antidynamo theorem under the presence of non-uniform electric conductivity

G. Rüdiger<sup>1,2\*</sup> and M. Schultz<sup>1</sup>

<sup>1</sup>Leibniz-Institut für Astrophysik Potsdam, An der Sternwarte 16, 14482 Potsdam, Germany

<sup>2</sup>University of Potsdam, Institute of Physics and Astronomy, Karl-Liebknecht-Str. 24-25, 14476 Potsdam, Germany

Received 01 July 2021, accepted later

Published online later

**Key words** MHD, Taylor-Couette flow, antidynamo theorem

Laminar electrically conducting Couette flows with the hydrodynamically stable quasi-Keplerian rotation profile and non-uniform conductivity are probed for dynamo instability. In spherical geometry the equations for the poloidal and the toroidal field components completely decouple, resulting in free decay, regardless of the spatial distribution of the electric conductivity. In cylindrical geometry the poloidal and toroidal components do not decouple, but here also we do not find dynamo excitations for the cases that the electric conductivity only depends on the radius or – much more complex – that it only depends on the azimuthal or the axial coordinate. The transformation of the plane-flow dynamo model of Busse & Wicht (1992) to cylindrical or spherical geometry therefore fails. It is also shown that even the inclusion of axial flows of both directions does *not* support the dynamo mechanism. The Elsasser toroidal-velocity antidynamo theorem, according to which dynamos without any radial velocity component cannot work, is thus not softened by non-uniform conductivity distributions.

Copyright line will be provided by the publisher

## 1 Introduction

It was demonstrated by Busse & Wicht (1992) that a large-scale magnetic field can be excited as a slab dynamo formed by a plane laminar shear flow and an electric conductivity which is sinusoidally modulated in the stream-wise direction. The flow becomes supercritical for rather large magnetic Reynolds numbers of  $O(10^4 \dots 5)$ , which can be optimized when the perturbation scale of the magnetic field approaches the scale of the conductivity variations, where the latter may exceed the thickness of the slab. If, on the other hand, the electric conductivity varied crosswise rather than streamwise no dynamo effect was found by the authors.

This raises the question of whether this positive result can be transformed to cylindrical and/or spherical geometry. If yes then a dynamo should also work for differential rotation of a fluid of non-uniform electric conductivity. The dynamo action should be possible for non-rigidly rotating cylinders or spheres with non-uniform conductivity distribution in the azimuthal direction. It is known, however, that spherical dynamos with only toroidal internal flows do not exist for uniform conductivity distribution (Elsasser 1946; Ivers & James 1988b; Kaiser & Busse 2017).

In this case differential rotation is not enough to form a dynamo mechanism but, as suggested by Gailitis (1970), pure meridional flow should be enough for sufficiently large magnetic Reynolds number of the flow (Latter & Ivers 2010; Moss 2006). Dudley & James (1989) demonstrated how the addition of differential rotation to the meridional

flow can strongly reduce the critical magnetic Reynolds number for suitable amplitude ratios of the flow components.

One can easily show that for spheres the toroidal-velocity antidynamo theorem also holds for non-uniform conductivity distribution. The induction equation for a laminar magnetized fluid with a finite magnetic resistivity  $\eta = 1/\mu\sigma$  (with  $\sigma$  as its electric conductivity) is

$$\frac{\partial \mathbf{B}}{\partial t} = \text{curl}(\mathbf{u} \times \mathbf{B} - \eta \text{curl} \mathbf{B}) \quad (1)$$

with  $\text{div} \mathbf{u} = \text{div} \mathbf{B} = 0$  for an incompressible fluid and  $\mathbf{u}$  as its velocity.  $\mathbf{B}$  is the magnetic field; here the magnetic resistivity is not necessarily uniform. The question is whether for given mean flow this equation, which is homogeneous in the magnetic field, has eigenvalues with marginal growth rates.

Following the method demonstrated in the textbook of Krause & Rädler (1980), the induction equation in spherical geometry is split into poloidal  $\text{curl} \mathbf{A}_{\text{tor}}$  and toroidal  $\mathbf{B}_{\text{tor}}$  components

$$\mathbf{A}_{\text{tor}} = -\mathbf{r} \times \nabla S, \quad \mathbf{B}_{\text{tor}} = -\mathbf{r} \times \nabla T, \quad (2)$$

with  $\mathbf{r}$  as the radial vector  $\mathbf{r} = (r, 0, 0)$  in spherical geometry. The result is two equations for  $S$  and  $T$ . Here only the relation

$$\frac{\partial S}{\partial t} + \Omega \frac{\partial S}{\partial \phi} - \eta \Delta S = U_{\text{ind}} \quad (3)$$

for the poloidal field component  $S$  must be considered, where  $\Omega$  is the (non-uniform) rotation rate of the sphere.

\* E-mail: GRuediger@aip.de

The right-hand side of this equation describes the induction by the mean circulation  $\mathbf{u}^m$ , i.e.

$$\mathcal{L}U_{\text{ind}} = -\mathbf{r} \cdot \text{curl} \mathbf{u}^m \times \mathbf{B}. \quad (4)$$

The operators

$$\begin{aligned} \Delta &= \frac{1}{r^2} \left( \frac{\partial}{\partial r} \left( r^2 \frac{\partial}{\partial r} \right) + \mathcal{L} \right), \\ \mathcal{L} &= \frac{1}{\sin \theta} \frac{\partial}{\partial \theta} \left( \sin \theta \frac{\partial}{\partial \theta} \right) + \frac{1}{\sin^2 \theta} \frac{\partial^2}{\partial \phi^2} \end{aligned} \quad (5)$$

are well-known. From Eq. (4) one finds the explicit formulation

$$\begin{aligned} \mathcal{L}U_{\text{ind}} &= -\nabla(ru_r) \cdot \mathbf{r} \times \nabla T - \mathbf{u}^m \nabla \mathcal{L}S + \\ &+ u_r(r\Delta S + \nabla \frac{\partial}{\partial r}(rS)). \end{aligned} \quad (6)$$

The striking result is that only the first term of the right-hand side of this relation is able to couple the toroidal field with Eq. (3), but this term vanishes for  $u_r = 0$ . Without this source term the relation (3) is homogeneous in  $S$  and only describes the decay of this field component, regardless of the actual form of the function  $\eta$  (Ivers & James 1988a). A self-maintaining nonturbulent dynamo in spherical geometry is thus only possible for flows with finite radial component, i.e. including meridional flows. This is the well-known antidynamo theorem, which obviously also holds for non-uniform distributions with  $\eta > 0$ . The transformation to spherical geometry of the plane dynamo model of Busse & Wicht (1992) that relies on streamwise  $\eta$ -modulation between two narrow plates is thus not possible. Kaiser & Busse (2017) have shown that this toroidal-velocity antidynamo theorem also survives up to a certain nonradial resistivity variation which decreases for increasing magnetic Reynolds numbers. The existence of this limit characterizes the robustness of the antidynamo theorem; dynamo excitation, therefore, is not excluded by this analysis for sufficiently large resistivity variations.

This might support the idea of Rogers & McElwaine (2017) that a dynamo can basically work in the thin stably stratified atmosphere of a hot Jupiter on the basis of strong conductivity variations due to the heating of the near host star. According to the findings of the present paper, however, even this dynamo can only operate under the presence of differential rotation *and* meridional circulation. Detailed calculations of the wind system in ultra-hot Jupiters have been published by Tan & Komacek (2019).

For non-uniform magnetic resistivity the induction equation reads

$$\frac{\partial \mathbf{B}}{\partial t} = \text{curl}(\mathbf{u} \times \mathbf{B}) + \eta \Delta \mathbf{B} - \nabla \eta \times \text{curl} \mathbf{B} \quad (7)$$

(Giesecke et al. 2010; Rogers & McElwaine 2017). It has been argued that the last term of this equation can formally be considered as a new alpha-effect term allowing for dynamo operation. However, this term is perpendicular to the electric current  $\text{curl} \mathbf{B}$ , while the corresponding term by an alpha effect is parallel to  $\text{curl} \mathbf{B}$ . One can show that one of

the main consequences of this last term is the advection of magnetic field in the direction of  $\nabla \eta$ . It is

$$\nabla \eta \times \text{curl} \mathbf{B} = \text{curl}(\nabla \eta \times \mathbf{B}) + \nabla(\nabla \eta \cdot \mathbf{B}) + \dots, \quad (8)$$

where the dots represent a tensor formed with second derivatives of  $\eta$ , i.e.  $(\Delta \eta \delta_{ij} - 2\eta_{,ij})B_j$ . The first term on the right-hand side of this equation describes advection of the field antiparallel to  $\nabla \eta$  (see Eq. (1)), which is, if too strong, known to suppress dynamo action, see Krause & Rädler (1980), Brandenburg et al. (1992) and Gressel et al. (2022). The remaining terms also cannot play the role of an alpha effect. The existence of an alpha effect always requires the existence of a pseudo-scalar or a pseudo-tensor.

It makes sense to inspect the radial component of (7) in spherical coordinates, i.e.

$$\begin{aligned} \frac{\partial B_r}{\partial t} + \Omega \frac{\partial B_r}{\partial \phi} &= \eta \left( \frac{1}{r} \frac{\partial^2}{\partial r^2} r B_r + \frac{1}{r^2} \frac{\partial^2 B_r}{\partial \theta^2} + \right. \\ &+ \frac{1}{r^2 \sin^2 \theta} \frac{\partial^2 B_r}{\partial \phi^2} + \frac{\cot \theta}{r^2} \frac{\partial B_r}{\partial \theta} + \frac{2}{r} \frac{\partial B_r}{\partial r} + \frac{2B_r}{r^2} \left. \right) - \\ &- \frac{1}{r^2} \frac{\partial \eta}{\partial \theta} \left( \frac{\partial}{\partial r} r B_\theta - \frac{\partial B_r}{\partial \theta} \right) + \\ &+ \frac{1}{r^2 \sin \theta} \frac{\partial \eta}{\partial \phi} \left( \frac{1}{\sin \theta} \frac{\partial B_r}{\partial \phi} - \frac{\partial}{\partial r} r B_\phi \right) \end{aligned} \quad (9)$$

All terms due to a meridional circulation have been cancelled. We note for the last two lines of this expression that the  $\nabla$ -terms of (8) appear. For strong shear the combination of  $\partial \eta / \partial \phi$  with  $B_\phi$  should make the strongest effect. A radial gradient of the resistivity does not appear explicitly.

## 2 Cylindrical geometry

The negative conclusion for spherical geometry cannot automatically be transformed to cylindrical geometry. A special situation exists for cylindrical geometry as the operator  $\text{curl} \text{curl}$  combines various magnetic field components, i.e.

$$\begin{aligned} \frac{\partial B_R}{\partial t} + \Omega \frac{\partial B_R}{\partial \phi} &= \eta \left( \frac{\partial}{\partial R} \left( \frac{1}{R} \frac{\partial}{\partial R} (R B_R) \right) + \frac{\partial^2 B_R}{\partial z^2} + \right. \\ &+ \frac{1}{R^2} \frac{\partial^2 B_R}{\partial \phi^2} - \frac{2}{R^2} \frac{\partial B_\phi}{\partial \phi} \left. \right) + \dots, \end{aligned} \quad (10)$$

now written in cylindrical coordinates  $(R, \phi, z)$ . Obviously, in contrast to (9), for nonaxisymmetric fields a coupling exists between the azimuthal and the radial field components which might be able to create a dynamo in a similar sense as the  $\Omega \times \mathbf{J}$  effect in turbulent dynamo theory does. The latter is part of the eddy diffusivity tensor containing the linear-in- $\Omega$  influence on the magnetic dissipation. It is thus necessary to find out whether for cylindrical models the combination of differential rotation and non-uniform electric conductivity can lead to dynamo instability

### 2.1 The model

Distances and wave numbers may be normalized with the outer cylinder radius  $R_0$ , and the inner cylinder is  $r_{\text{in}} R_0$ .

The rotation and other frequencies are normalized with the rotation rate  $\Omega_{\text{in}}$  of the inner cylinder; the rotation rate of the outer cylinder is  $\mu\Omega_{\text{in}}$ . The rotation law may be written as

$$\Omega(R) = a_{\Omega} + \frac{b_{\Omega}}{R^2} \quad (11)$$

with

$$a_{\Omega} = \frac{\mu - r_{\text{in}}^2}{1 - r_{\text{in}}^2}, \quad b_{\Omega} = \frac{1 - \mu}{1 - r_{\text{in}}^2} r_{\text{in}}^2. \quad (12)$$

Here  $\mu = \Omega_{\text{out}}/\Omega_{\text{in}}$  is the ratio of the rotation rates of the outer and inner cylinders. For  $\mu = r_{\text{in}}^{1.5}$  the cylinders rotate according to the Kepler law, i.e.  $\mu = 0.35$  for  $r_{\text{in}} = 0.5$ . This rotation law is flat enough to avoid the flow becoming centrifugally unstable. The Rayleigh limit for  $r_{\text{in}} = 0.5$  is  $\mu = 0.25$ , above which the flows are stable. The magnetic Reynolds number of the rotation is defined as

$$\text{Rm} = \frac{\Omega_{\text{in}} R_0^2}{\eta_0}, \quad (13)$$

where  $\eta_0$  is a characteristic value of the resistivity defined by the definition of the  $\eta$ -profile. The magnetic field vector in cylindrical coordinates is  $\mathbf{B} = (A, B, B_z)$ . The equations are solved by means of the Fourier series  $A = \sum_m A_m(R) \exp i(kz + m\phi + \omega t)$  and  $B = \sum_m B_m(R) \exp i(kz + m\phi + \omega t)$ , while the axial field  $B_z$  is always substituted by means of the divergency condition. The solutions are assumed to be periodic along the rotation axis, with  $k$  as the wave number (a parameter) in this direction.  $\omega$  is the eigenvalue of the system, with its real part as the azimuthal drift rate and its negative imaginary part as the growth rate. Negative growth rate indicates decay of the magnetic pattern while vanishing growth rate marks neutral instability. In case of self-excitation the wave number  $k$  can be used to find the optimal excitation condition.

The eigenfunctions and the eigenvalues fulfil the symmetry conditions

$$A_{-m} = A_m^*, \quad B_{-m} = B_m^* \quad \text{if} \quad \omega_{-m} = -\omega_m^*, \quad (14)$$

where an asterisk represents the conjugate complex expression.

To normalize the growth rate with the diffusion time we have simply to write

$$\omega_{\text{gr}} = -\text{Rm} \omega^{\text{I}}. \quad (15)$$

Here the notation is  $\omega = \omega^{\text{R}} + i\omega^{\text{I}}$ . If  $\omega_{\text{gr}}$  does not depend on Rm and is of order unity then growth (or decay) of the modes are only directed by the diffusion scale. Negative values of (15) indicate decaying magnetic fields. All plots in this paper are using the growth rates described in these units. The same is true for the drift rates  $d\phi/dt = -\omega_{\text{dr}}$  with

$$\omega_{\text{dr}} = \text{Rm} \omega^{\text{R}}. \quad (16)$$

Hence,  $\omega_{\text{dr}} < 0$  implies azimuthal drift in the positive direction.

For comparison both the decay and drift rates of infinite cylinders with uniform resistivity have been calculated with

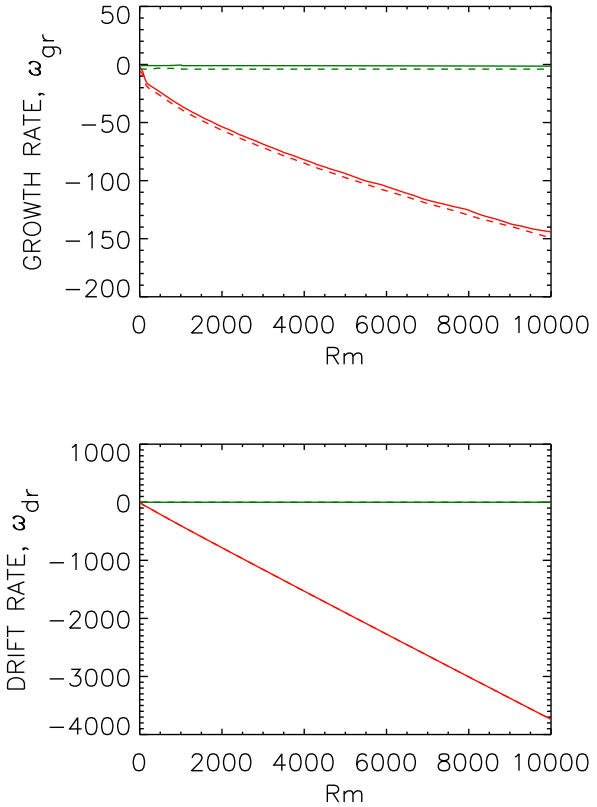


**Fig. 1** Reference plots: decay rates (top) and drift rates (bottom) in units of the diffusion time for uniform  $\eta$  and for  $m = 0$  (green) and for  $m = 1$  (red). Two different wave numbers  $k = 1$  (solid),  $k = 2$  (dashed).  $r_{\text{in}} = 0.5$ ,  $\mu = 0.35$  (Keplerian rotation), and perfectly conducting boundary conditions.

the results presented by Fig. 1. The upper panel concerns the decay of the modes with  $m = 0$  (green lines) and  $m = 1$  (red lines) for two different wave numbers  $k = 1$  (solid lines) and  $k = 2$  (dashed lines). Axisymmetric magnetic fields decay with the diffusion time scale, hence the influence of the differential rotation can be neglected. The non-axisymmetric mode with  $m = 1$  decays even faster. Without rotation the resulting growth rates for  $k = 1$  are  $\omega_{\text{gr}} = -1$  for axisymmetric fields and  $\omega_{\text{gr}} = -2.83$  for nonaxisymmetric fields with  $m = 1$ . For  $k = 2$  the corresponding numbers are  $\omega_{\text{gr}} = -4$  and  $\omega_{\text{gr}} = -5.83$ . In contrast to the decay law for  $m = 0$ , for  $m = 1$  the influence of the magnetic Reynolds number is strong so that the physical decay rate scales with the rotation rate,  $\omega_{\text{gr}} \propto -\Omega$ . The decay time of nonaxisymmetric fields is strongly reduced by rotational shear, independent of its sign. As the winding-up of the field lines by the differential rotation leads to shorter scales, for rapid rotation the decay time becomes shorter (Krause & Rädler 1980). For high magnetic Reynolds numbers nonaxisymmetric fields decay about  $\sqrt{\text{Rm}}$  times faster than axisymmetric fields.

The azimuthal drift of an axisymmetric field, of course, vanishes while nonaxisymmetric fields basically drift by the action of the differential rotation (bottom panel of Fig 1). The drift frequency for large Rm corresponds to the rotation rate of the outer cylinder, i.e.  $\mu\Omega_{\text{in}}$ . As formulated by Elsasser (1946), assuming uniform conductivity “for toroidal flow the induction effect consists in oscillatory changes of the field amplitudes superposed upon the slow, general decay of the field”.

In the following we shall demonstrate that these results are only slightly modified if the molecular resistivity  $\eta$  is no longer uniform. Here we distinguish between models with radial gradients and models with azimuthal gradients. Axial gradients of  $\eta$  are not considered in this paper as Busse & Wicht (1992) also did not find dynamo excitation for such models.

## 2.2 Radius-dependent conductivity

We start by considering a differentially rotating fluid in a cylindrical container with a radius-dependent magnetic resistivity. We write  $\eta = \eta_0\eta(R)$  with  $\eta(R) = R^{-\mu_\eta}$  (hence  $\eta(1) = 1$ ), where the profile parameter  $\mu_\eta$  can have both signs. For positive values the electric conductivity grows outward. The model is rather simple as the radius-dependent magnetic resistivity does not lead to complicated mode couplings as in the model by Busse & Wicht (1992) or as in our models with azimuth-dependent or  $z$ -dependent  $\eta$  profiles. The equation system for four differential equations of first order is used as formulated by Shalybkov et al. (2002), i.e.

$$\frac{d\tilde{A}_m}{dR} - \left(k^2 + \frac{m^2}{R^2}\right)A_m - \frac{i\text{Rm}}{\eta(R)}(\omega + m\Omega(R))A_m - \frac{2im}{R^2}B_m = 0, \quad (17)$$

$$\begin{aligned} \frac{d\tilde{B}_m}{dR} - \frac{\mu_\eta\tilde{B}_m}{R} - \left(k^2 + \frac{m^2}{R^2}\right)B_m - \\ - \frac{i\text{Rm}}{\eta(R)}(\omega + m\Omega(R))B_m + \\ + (2 + \mu_\eta)\frac{imA_m}{R^2} - 2\frac{\text{Rm}b_\Omega}{\eta(R)R^2}A_m = 0 \end{aligned} \quad (18)$$

with

$$\tilde{A}_m = \frac{dA_m}{dR} + \frac{A_m}{R}, \quad \tilde{B}_m = \frac{dB_m}{dR} + \frac{B_m}{R}. \quad (19)$$

The boundary conditions for these equations are  $A_m = \tilde{B}_m = 0$  for perfectly conducting walls at  $R = r_{\text{in}}, 1$  or

$$\left(k^2 + \frac{m^2}{R^2}\right)B_m - \frac{im\tilde{A}_m}{R} = 0 \quad (20)$$

for vacuum conditions. In this case it is also

$$kA_m - \left(\tilde{A}_m + \frac{imB_m}{R}\right) \left(\frac{m}{kR} + \frac{I_{m+1}(kR)}{I_m(kR)}\right) = 0 \quad (21)$$

at  $R = r_{\text{in}}$  and

$$kA_m - \left(\tilde{A}_m + \frac{imB_m}{R}\right) \left(\frac{m}{kR} - \frac{K_{m+1}(kR)}{K_m(kR)}\right) = 0 \quad (22)$$

at  $R = 1$  (Rüdiger et al. 2018). We note that the modified Bessel functions  $I$  and  $K$  satisfy  $I_{-m} = I_m$  and  $K_{-m} = K_m$ . Sometime also pseudo-vacuum conditions (vertical fields)  $B_m = \tilde{A}_m = 0$  have been used at  $R = r_{\text{in}}, 1$ .

The decay rates for two models with Keplerian rotation and with radial  $\eta$ -gradients of opposite signs are given in Fig. 2. The free axial wave numbers have been varied between  $k = 0.1$  and  $k = 1$ , but the curves are almost identical. Magnetic modes with different wave numbers decay with the same rate – except for  $\text{Rm} = 0$  where the modes with larger wave number (here  $k = 1$ ) decay faster. The magnetic Reynolds number of the rotation is assumed to increase up to the very large values  $\text{Rm} \lesssim 10^4$ . As expected for nonaxisymmetric fields under the influence of differential rotation, the decay rate grows with growing magnetic Reynolds numbers; the decay frequency is thus proportional to the rotation rate hence  $\tau_{\text{dec}} \propto \tau_{\text{in}}$  with  $\tau_{\text{in}}$  as the rotation period of the inner cylinder. Short time scales are produced by the winding-up of the field lines by the non-uniform rotation, which decay faster the larger the value of Rm is. The decay rates for  $\eta$  increasing outwards or decreasing outwards do not differ basically. The influence of the sign of the  $\eta$ -gradient on the decay times is obviously weak. As it should, the decay is (slightly) faster for negative gradients, i.e. for  $\mu_\eta > 0$ . The drift rates (not shown) in both cases are almost identical with the values shown in the lower panel of Fig. 1. Independently of the basically different radial  $\eta$ -profiles the nonaxisymmetric field pattern always drifts with the rate  $\Omega_{\text{out}}$  for large Rm.

The result is that a radial non-uniformity of conductivity even for large magnetic Reynolds numbers does not lead to dynamo action (Ivers & James 1988a). Figure 2 shows that a nonaxisymmetric field also cannot be maintained by differential rotation alone. The toroidal-velocity antidynamo theorem obviously also holds for cylindrical geometry and arbitrary radial  $\eta$ -gradients. The curves do not show any indication that the trends are changed for higher magnetic Reynolds numbers. In agreement with Kaiser & Busse (2017) we do not find evidence for dynamo action of differential rotation in combination with radial  $\eta$ -gradients of either sign.

## 3 Azimuth-dependent conductivity

Models with nonradial variation of the  $\eta$ -profile are more complex. The reason is that in the nonradial coordinates  $z$  and  $\phi$  the solutions are developed into Fourier modes, and for resistivities varying in these directions the modes couple, always producing an infinite series. Here we shall only provide solutions of the dynamo equation (1) for  $\eta$  as a function of the azimuth  $\phi$ .

The azimuthal variation of the magnetic resistivity may be written as

$$\eta = \eta_0(1 - \kappa \cos \phi), \quad (23)$$



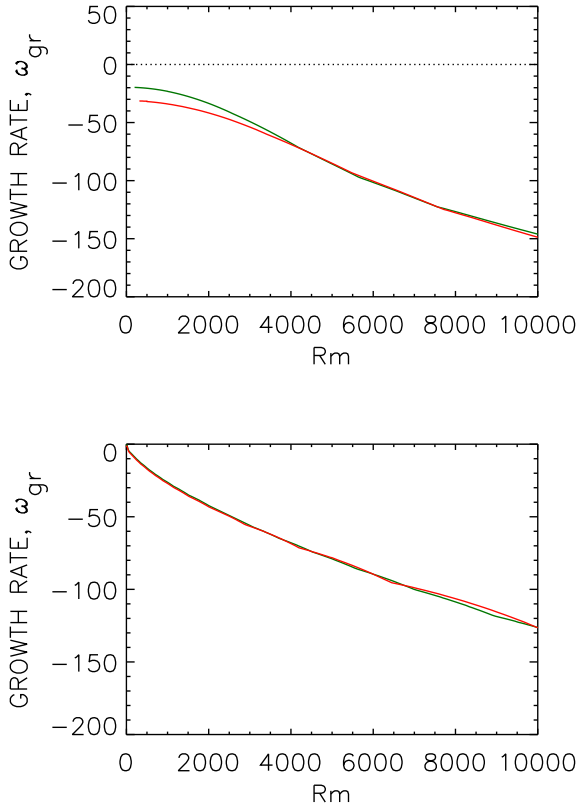


**Fig. 2** Decay rates of the nonaxisymmetric mode ( $m = 1$ ) in units of the diffusion time for two models of  $\eta = \eta(R)$ . Top:  $\mu_\eta = 10$  (conductivity grows outward), insulating walls; Bottom:  $\mu_\eta = -3$  (conductivity grows inward), perfectly conducting walls. Wave numbers  $k = 0.1$  (green),  $k = 1$  (red).  $r_{\text{in}} = 0.5$ ,  $\mu = 0.35$  (Keplerian rotation).

**Table 1** Coefficients  $\kappa_n$  and  $\bar{\kappa}_n$  for  $\kappa = 0.5$  and  $\kappa = 0.9$ .

mode $n$	$\kappa_n(0.5)$	$\bar{\kappa}_n(0.5)$	$\kappa_n(0.9)$	$\bar{\kappa}_n(0.9)$
-3	0.019	0.022	0.25	0.56
-2	0.072	0.083	0.39	0.96
-1	0.27	0.31	0.63	1.44
0	0	1.15	0	2.29
1	-0.27	0.31	-0.63	1.44
2	-0.072	0.083	-0.39	0.96
3	-0.019	0.022	-0.25	0.56

where the coefficient  $\kappa$  may vary between 0 and 1. The value  $\eta_0$  is the average over the azimuth. The ratio of the maximum value of  $\eta$  and its minimum is simply  $(1 + \kappa)/(1 - \kappa)$ , so that it approaches large values for  $\kappa \rightarrow 1$ .

Ansatz (23) describes the consequences of a heating of the cylinder at a phase zero and a cooling at the opposite phase  $\pi$ . One could also work with higher azimuthal frequencies by replacing  $\cos \phi$  in (23) by  $\cos N\phi$ , but here we always take  $N = 1$ . In all cases with  $\kappa \neq 0$  the magnetic modes with the azimuthal wave number  $m$  are coupled, so

that an infinite set of equations results. The coupling coefficients are

$$\begin{aligned} \kappa_n &= \frac{i\kappa}{2\pi} \int_0^{2\pi} \frac{\sin \phi e^{in\phi}}{1 - \kappa \cos \phi} d\phi, \\ \bar{\kappa}_n &= \frac{1}{2\pi} \int_0^{2\pi} \frac{e^{in\phi}}{1 - \kappa \cos \phi} d\phi. \end{aligned} \quad (24)$$

The  $\kappa_n$  and  $\bar{\kappa}_n$  are real numbers with  $\kappa_{-n} = -\kappa_n$  and  $\bar{\kappa}_{-n} = \bar{\kappa}_n$ . For  $\kappa = 0$  we have  $\bar{\kappa}_0 = 1$  and all other  $\bar{\kappa}_n$  vanish. Analytically, for  $\kappa \gg 1$  it is  $\kappa_{\pm 1} \simeq \mp \kappa/2$  and  $\bar{\kappa}_{\pm 1} \simeq \kappa/2$

According to Cowling's theorem we must consider the growth or decay of a nonaxisymmetric magnetic field. Written with the definitions (19) the resulting equation system for growth or decay of the mode with  $m = 1$  (defined by  $M = 0$ ) is

$$\begin{aligned} \frac{d\tilde{A}_m}{dR} &- (k^2 + \frac{m^2}{R^2})A_m - \frac{2im}{R^2}B_m - \\ &- iRm \sum_{n=1-M}^{1+M} \bar{\kappa}_{n-m}(\omega + n\Omega(R) + kU(R))A_n + \\ &+ \sum_{n=1-M}^{1+M} \kappa_{n-m} \left( \frac{nA_n}{R^2} + \frac{i\tilde{B}_n}{R} \right) = 0 \end{aligned} \quad (25)$$

and

$$\begin{aligned} \frac{d\tilde{B}_m}{dR} &- (k^2 + \frac{m^2}{R^2})B_m + \frac{2im}{R^2}A_m - \\ &- iRm \sum_{n=1-M}^{1+M} \bar{\kappa}_{n-m}(\omega + n\Omega(R) + kU(R))B_n - \\ &- 2Rm \frac{b_\Omega}{R^2} \sum_{n=1-M}^{1+M} \bar{\kappa}_{n-m}A_n = 0 \end{aligned} \quad (26)$$

formulated for all  $m$  with  $1-M \leq m \leq 1+M$ . The number  $M$  limits the equation system which is solved if the eigenvalues no longer depend on the choice of  $M$ . It is also possible to consider the stability of a higher nonaxisymmetric mode, but here we focus on  $m = 1$ . The numerical results in Fig. 3 for  $\kappa = 0.5$  and with the approximation  $M = 1$  for growth rates and drift rates (both normalized with the diffusion frequency) of the eigensolutions are plotted for our standard container ( $r_{\text{in}} = 0.5$ ) and for Keplerian rotation. The resistivity varies in accordance with (23) without any radial variation. The plot shows the eigenfrequencies for the two wave numbers  $k = 1$  and  $k = 2$ . The results are surprising. The modes are always decaying. However, in contrast to the eigenvalues for isolated nonaxisymmetric modes and axisymmetric resistivity with the characteristic  $Rm$  behavior shown in Fig. 2, the resulting growth rates in units of the diffusion rate do *not* depend on the magnetic Reynolds number (upper panel) and the decaying patterns do *not* drift in azimuthal direction (lower panel). The non-axisymmetric  $\eta$ -profile stops the azimuthal drift of the non-axisymmetric modes and the influence of the differential rotation on the normalized decay rate disappears. Due to the

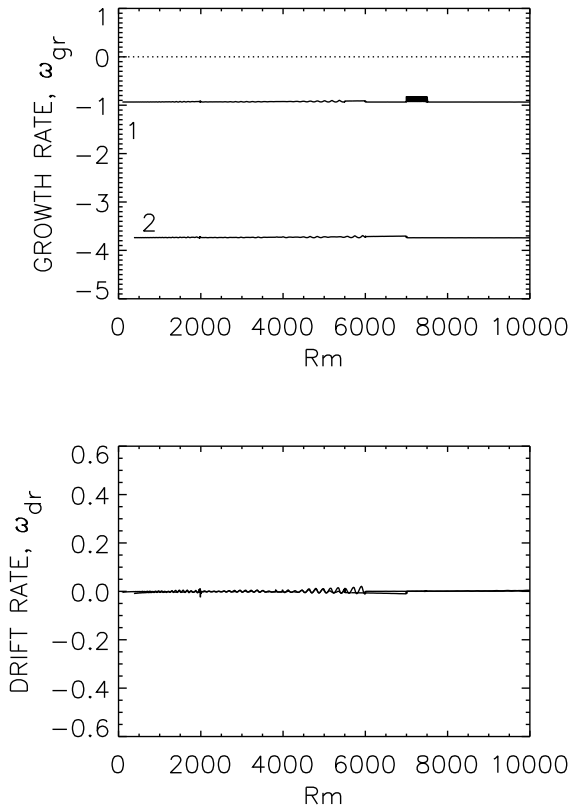


**Fig. 3** Growth rate (top) and drift rate (bottom) in units of the diffusion rate for two values of the free axial wave number ( $k = 1$  and  $k = 2$ , marked) for azimuth-dependent electric conductivity.  $r_{\text{in}} = 0.5$ ,  $\mu = 0.35$  (Keplerian rotation).  $\kappa = 0.5$ ,  $m = 1$ ,  $M = 1$ . The dotted line denotes marginal stability. Perfectly conducting boundary conditions.

nonaxisymmetric  $\eta$ -profile the  $m = 1$  mode is always coupled to the  $m = 0$  mode which does not feel the influence of the differential rotation (see Fig. 2, upper panel) and decays only slowly. By the coupling of all the azimuthal modes the  $m = 1$  mode then also decays as slowly as the  $m = 0$  mode (see Fig. 3, upper panel)<sup>1</sup>.

The upper panel of Fig. 4 shows the growth rates for Keplerian rotation which result from the approximations with  $M = 1$  and  $M = 2$  for a medium gap with  $r_{\text{in}} = 0.5$  and two narrow gaps with  $r_{\text{in}} = 0.9$  and  $r_{\text{in}} = 0.95$ . The number of equations strongly grows for growing  $M$ . For  $M = 1$  the solver works for twelve equations while for  $M = 2$  twenty equations are concerned. Nevertheless, the results are very similar, i.e. the growth rates are always negative with almost the same numerical value of order unity. Hence, the modes decay with the diffusion time scale independent of the geometry of the tube and independent of the magnetic Reynolds number  $Rm$ . We note that the diffusion

<sup>1</sup> This statement can be proved by solving the system (25) and (26) for  $\kappa = 0$  and  $M = 0$  which exactly reproduces the red lines in Fig. 2 for the decay of the nonaxisymmetric  $m = 1$  mode with uniform resistivity.

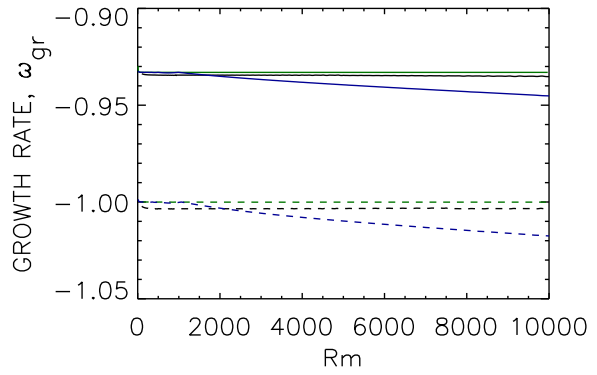


**Fig. 4** Growth rates normalized with the diffusion frequency for a nonaxisymmetric magnetic field with  $m = 1$ . Azimuth-dependent electric conductivity with  $\kappa = 0.5$ .  $M = 1$  (solid) and  $M = 2$  (dashed). Three different gaps between the cylinders:  $r_{\text{in}} = 0.5$  (black),  $r_{\text{in}} = 0.9$  (green),  $r_{\text{in}} = 0.95$  (blue).  $\mu = r_{\text{in}}^{1.5}$  (Keplerian rotation),  $k = 1$ . As in Fig. 3 the drift rates vanish. Perfectly conducting boundary conditions.

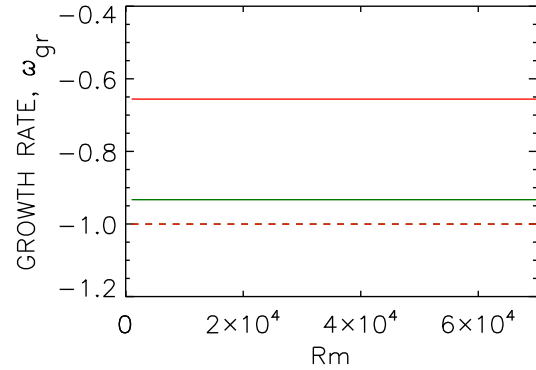


**Fig. 5** Similar to Fig. 4 but for very large magnetic Reynolds numbers  $Rm$  and with  $\kappa = 0.5$  (green) and  $\kappa = 0.95$  (red).  $M = 1$  (solid),  $M = 2$  (dashed). For  $M = 2$  the two dashed lines (red and green) are identical.  $r_{\text{in}} = 0.9$ ,  $\mu = 0.85$  (Keplerian rotation),  $k = 1$ . As in Fig. 3 the drift rates vanish in all cases. Perfectly conducting boundary conditions.

time scale is formed with the outer cylinder radius  $R_0$ ; the choice of  $r_{\text{in}}$  does not play a role for the decay rate of the (nonaxisymmetric) mode.

In both approximations the decay rates behave very similarly. The main difference is a slightly higher decay rate if  $M = 2$  which is *unity for all models* if  $Rm$  is small. While for the wider gap the curves are strictly horizontal, there may be a little slope for the narrow gaps (see below). The lower panel of Fig. 4 again demonstrates that the considered nonaxisymmetric field with  $m = 1$  does not drift in the azimuthal direction during its decay. The system always behaves very similar to the behavior of the mode  $m = 0$ .

The curves in Fig. 4 do not completely exclude the possibility that for narrow gaps the negative growth rates may

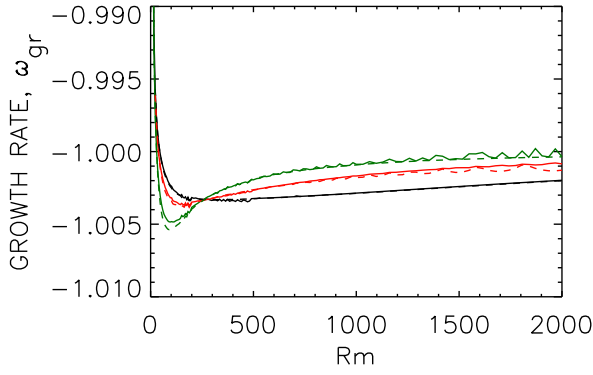


**Fig. 6** Growth rates in units of the diffusion rate for various values of the axial flow  $-0.5 \leq \hat{U} \leq 0.5$  for  $k = 1$  and azimuth-dependent electric conductivity. Solid lines:  $\hat{U} > 0$ , dashed lines:  $\hat{U} < 0$ . Green:  $|\hat{U}| = 0.5$ , red:  $|\hat{U}| = 0.25$ , black:  $|\hat{U}| = 0.1$ .  $r_{\text{in}} = 0.5$ ,  $\mu = 0.35$  (Keplerian rotation).  $\kappa = 0.5$ ,  $M = 2$ . Perfectly conducting boundaries.

change their sign for much higher  $Rm$  and a dynamo could start to operate there. For the narrow gap with  $r_{\text{in}} = 0.9$  we thus evaluated with Keplerian rotation the eigenfrequencies also for very large magnetic Reynolds numbers and for the two resistivity profiles with  $\kappa = 0.5$  and  $\kappa = 0.95$ .  $\kappa = 0.5$  describes an azimuthal peak-to-peak variation of the molecular conductivity by a factor of 3 and  $\kappa = 0.95$  by a factor of 39. The latter model (thin gap, massive conductivity variations, large magnetic Reynolds numbers) may well approach the assumptions used by Busse & Wicht (1992) in flat geometry. But in cylindrical geometry only negative growth rates are provided for  $Rm \leq 10^5$ , independent of the actual value of  $\kappa$  (Fig. 5, upper panel). The nonaxisymmetric mode with  $m = 1$  just decays with the diffusion time of the purely axisymmetric mode with  $m = 0$ . The combination of differential rotation and non-uniform molecular conductivity in our calculations does not lead to positive growth rates, so that a dynamo does not exist here. Again the azimuthal drift of the magnetic pattern disappears as it does for the decay of the  $m = 0$  mode shown in the lower panel of Fig. 1.

We also briefly checked the action of an axial flow  $U(R)$  – independent of  $z$  – as a function of the radius for the induction equations (25) and (26). It is normalized with the azimuthal flow speed  $\Omega_{\text{in}} R_0$ , i.e.  $U(R) = u_z / \Omega_{\text{in}} R_0$  and its radial profile is simply put to

$$U(R) = \hat{U} \sin \frac{2(R - r_{\text{in}})\pi}{1 - r_{\text{in}}}. \quad (27)$$

Figure 6 demonstrates the irrelevance of such an axial flow (of both circulation regimes) for the dynamo mechanism, which is not surprising. Positive results can only be expected after inclusion of a radial flow but then we would confirm – or not – the results of Dudley & James (1989) for the ability of combined systems of differential rotation

and meridional circulations to solve the dynamo equation (1) with positive growth rates.

#### 4 Axial conductivity variations

It remains to probe axial profiles of the molecular resistivity to support dynamo action. This problem does not cover the transformation of the dynamo of Busse & Wicht (1992) to cylindrical or spherical geometry as they also denied the operation of such a dynamo in their model. Inspecting the equation system one finds a more complex instability problem. The last term of Eq. (8) for  $\eta = \eta(z)$  provides a coupling of the equations via  $B_z$ . If ever, the radial magnetic field is exclusively originated by the axial field rather than by the azimuthal field as it is the case for  $\eta = \eta(\phi)$ . The coupling is thus only weak for dynamos with weak axial fields as it is usually realized for dynamos with differential rotation. As nevertheless such a dynamo cannot be excluded new calculations must provide the consequences of profiles such as  $\eta = \eta(z)$ , see Marcotte et al. (2021).

The axial profile of the resistivity may be modeled by  $\eta = \eta_0(1 - \zeta \cos z)$ ,

where the free parameter  $\zeta$  describes the amplitude of the axial resistivity variations.  $\zeta = 1$  must naturally be excluded. The wave number of the resistivity variations with (28) is thus unity. The coefficients similar to (24) are

$$\begin{aligned} \kappa_n &= \frac{i\zeta}{2\pi} \int_0^{2\pi} \frac{\sin z e^{inz}}{1 - \zeta \cos z} dz, \\ \bar{\kappa}_n &= \frac{1}{2\pi} \int_0^{2\pi} \frac{e^{inz}}{1 - \zeta \cos z} dz. \end{aligned} \quad (29)$$

Again  $\kappa_n$  and  $\bar{\kappa}_n$  are real with  $\kappa_{-n} = -\kappa_n$  and  $\bar{\kappa}_{-n} = \kappa_n$ . The definitions

$$\tilde{A}_k = \frac{dA_k}{dR} + \frac{A_k}{R}, \quad \tilde{B}_k = \frac{dB_k}{dR} + \frac{B_k}{R} \quad (30)$$

are also parallel to the above notation. The resulting equations are

$$\begin{aligned} \frac{d\tilde{A}_k}{dR} &- (k^2 + \frac{m^2}{R^2})A_k - \frac{2im}{R^2}B_k - \\ &- iRm(\omega + m\Omega(R)) \sum_{\ell=k^*-K}^{k^*+K} \bar{\kappa}_{\ell-k} A_\ell \\ &= \sum_{\ell=k^*-K}^{k^*+K} \frac{\kappa_{\ell-k}}{\ell} \left( \frac{d\tilde{A}_\ell}{dR} + \frac{im\tilde{B}_\ell}{R} - \frac{2imB_\ell}{R^2} - \ell^2 A_\ell \right), \end{aligned}$$

and

$$\begin{aligned} \frac{d\tilde{B}_k}{dR} &- (k^2 + \frac{m^2}{R^2})B_k + \frac{2im}{R^2}A_k - \\ &- iRm(\omega + m\Omega(R)) \sum_{\ell=k^*-K}^{k^*+K} \bar{\kappa}_{\ell-k} B_\ell - \\ &- 2Rm \frac{b_\Omega}{R^2} \sum_{\ell=k^*-K}^{k^*+K} \bar{\kappa}_{\ell-k} A_\ell \\ &= \sum_{\ell=k^*-K}^{k^*+K} \frac{\kappa_{\ell-k}}{\ell} \left( \frac{im\tilde{A}_\ell}{R} - \frac{m^2 B_\ell}{R^2} - \ell^2 B_\ell \right), \end{aligned} \quad (31)$$

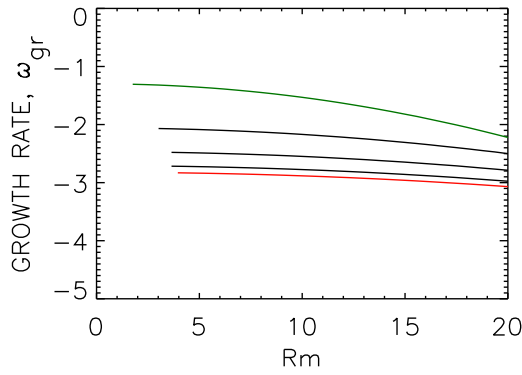


**Fig. 7** Growth rates for containers with the axial conductivity profile (28) for slow rotation. It is  $k^* = 2 r_{\text{in}} = 0.5$ ,  $\mu = 0.35$  (Keplerian rotation),  $m = 1$ . The  $\zeta$  varies from 0.9 (green) to  $\zeta = 0.1$  (red). Perfectly conducting boundary conditions.

formulated for all  $k$  with  $k^* - K \leq k \leq k^* + K$ . Although the  $k$ 's denote wave numbers they are here considered as real integers<sup>2</sup>. The system contains  $8K + 4$  equations with  $k^*$  as the central wave number. Because of the Cowling theorem only the stability of nonaxisymmetric fields is probed, hence  $m = 1$  is fixed.

We start with  $k^* = 2$  and  $K = 1$  so that a modal system with wave numbers  $k = 1$ ,  $k = 2$  and  $k = 3$  is considered. The wave number  $k = 1$  of the resistivity variation (28) is part of the spectrum. The remaining modes  $k = 2$  and  $k = 3$  are higher modes. Indeed, Fig. 7 demonstrates that for small  $\zeta$  and slow rotation the decay rates approach that for  $k = 1$  and *uniform* resistivity shown by Fig. 1 for the case of  $m = 1$ . Faster rotation seems to amplify the decay of the magnetic field.

The overall result of the calculations is that we do not find modes for any magnetic Reynolds number and/or for any value of  $\zeta$  as unstable, i.e. all growth rates become negative. Figure 8 demonstrates for nonaxisymmetric fields with  $m = 1$ , axial resistivity distribution and much higher Reynolds numbers that both the physical growth rate and the physical drift rate grow with growing rotation rate, similar to the decay mode with  $m = 1$  and  $\zeta = 0$  in Fig. 1 (red lines). Differential rotation obviously destabilizes the magnetic fields, i.e. they decay faster. On the other hand, the axial non-uniformity of the molecular conductivity slightly *stabilizes* the magnetic field in comparison to the same configuration with uniform conductivity.

Another example, Fig. 9, contains the growth rates and the drift rates for a fixed high value  $Rm = 2000$  for the three central wavenumbers  $k^* = 1.5$ ,  $k^* = 2$  and  $k^* = 3$ . For  $\zeta = 0$  and  $k^* = 2$  both the growth rate and the drift rate are identical to the numbers given in Fig. 1 for  $Rm = 2000$  while for  $\zeta = 0.5$  the values for  $Rm = 2000$  in the Figs. 8 and 9 coincide. For growing  $\zeta$  the absolute value

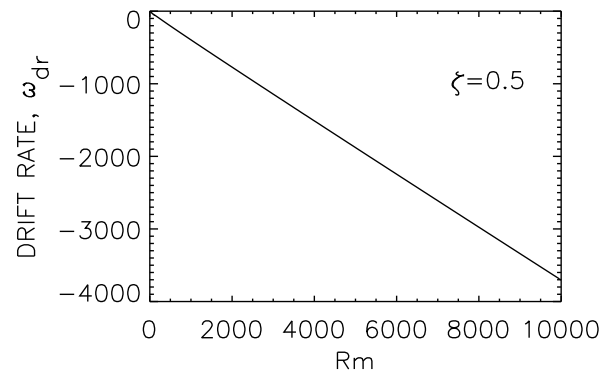
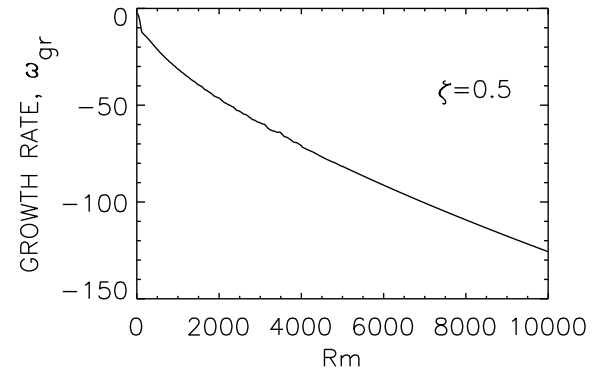


**Fig. 8** Growth rate (top) and drift rate (bottom) for containers with the periodic axial conductivity profile (28) with variation of  $Rm$  and for  $m = 1$ . The axial modulation of the resistivity is fixed to  $\zeta = 0.5$ . It is  $k^* = 2$ ,  $r_{\text{in}} = 0.5$ ,  $\mu = 0.35$  (Keplerian rotation), Perfectly conducting boundary conditions.

of the growth rate sinks while the drift rate remains almost constant. The differences of these values for different wave numbers  $k^*$  are very small. Obviously, the fastest decay of the magnetic field happens for  $\zeta = 0$ , i.e. if the resistivity in the cylinder is uniform.

Dynamos with differential rotation without meridional circulation have never been found in this study even not for models with non-uniform resistivity profiles.

## 5 Conclusion

We have shown by use of both spherical and cylindrical models that any dependence of the molecular resistivity  $\eta$  on the position  $x$  does not soften the toroidal-velocity antidynamo theorem of Elsasser (1946). Our laminar velocity fields do not possess radial components, and thus we do not find any dynamo self-excitation. Under the exclusive influence of various rotation laws the nonaxisymmetric  $m = 1$  mode *decays* for all the considered  $\eta$ -profiles and gap widths up to magnetic Reynolds numbers of  $10^5$ . The decay time runs the diffusion time scale for axisymmetric disturbances and with the rotation time for nonaxisymmet-

<sup>2</sup> We note that here the asterisk does not mean “complex conjugate”.



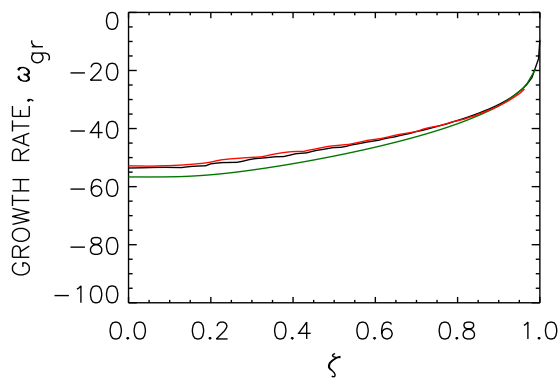


**Fig. 9** Growth rates for containers with the axial conductivity profile (28) for variation of  $\zeta$ . The magnetic Reynolds number is fixed to  $Rm = 2000$ . It is  $k^* = 1.5$  (red),  $k^* = 2$  (black) and  $k^* = 3$  (green).  $r_{in} = 0.5$ ,  $\mu = 0.35$  (Keplerian rotation),  $m = 1$ . We note that possible solutions for the exotic case  $\zeta = 1$  are excluded. Perfectly conducting boundary conditions.

ric disturbances (and fast rotation) almost independent of the amplitude of the azimuthal variation of the the  $\eta$ -profile and also independent of the differential rotation laws.

These findings should be of relevance for the idea that a hot exoplanet develops strong differences of the electric conductivity at their day-side and night-side with possible potential to form a magnetic dynamo system (Rogers & McElwaine 2017). Based on our results this would only be possible if the antidynamo theorem is overcome by inclusion of a radial flow component, but such complex flows can already generate nonaxisymmetric magnetic fields even without non-uniform molecular conductivity (Dudley & James 1989). For the operation of a laminar dynamo the radial flow component cannot successfully be replaced by gradients of the electric conductivity. The idea of Elsasser about resistivity variations is confirmed that “it does not seem plausible that this variation introduces phenomena that modify the theory in a fundamental way”.

**Acknowledgment** Axel Brandenburg (Stockholm), Rainer Hollerbach (Leeds) and Johannes Wicht (Göttingen) are cordially acknowledged for stimulating discussions.

## References

- Brandenburg A., Moss D., Tuominen I., 1992, in Harvey K. L., ed., *The Solar Cycle Vol. 27 of Astronomical Society of the Pacific Conference Series, Turbulent Pumping in the Solar Dynamo*. p. 536
- Busse F. H., Wicht J., 1992, *Geophysical and Astrophysical Fluid Dynamics*, 64, 135
- Dudley M. L., James R. W., 1989, *Proceedings of the Royal Society of London Series A*, 425, 407
- Elsasser W. M., 1946, *Physical Review*, 69, 106
- Gailitis A., 1970, *Magnitnaia Hidrodinamika*, p. 19

- Giesecke A., Nore C., Stefani F., Gerbeth G., Leorat J., Ludens F., Guermond J. L., 2010, *Geophysical and Astrophysical Fluid Dynamics*, 104, 505
- Gressel O., Rüdiger G., Elstner D., 2022, *Astron. Nachr.*, *subm.*
- Ivers D. J., James R. W., 1988a, *Geophysical and Astrophysical Fluid Dynamics*, 44, 271
- Ivers D. J., James R. W., 1988b, *Geophysical and Astrophysical Fluid Dynamics*, 40, 147
- Kaiser R., Busse F., 2017, *Geophysical and Astrophysical Fluid Dynamics*, 111, 355
- Krause F., Rädler K. H., 1980, *Mean-field magnetohydrodynamics and dynamo theory*. Pergamon Press
- Latter H., Ivers D., 2010, *Physics of Fluids*, 22, 066601
- Marcotte F., Gallet B., Pétrélis F., Gissinger C., 2021, *Physical Review E*, 104, 015110
- Moss D., 2006, *Geophysical and Astrophysical Fluid Dynamics*, 100, 49
- Rogers T. M., McElwaine J. N., 2017, *The Astrophysical Journal Letters*, 841, L26
- Rüdiger G., Gellert M., Hollerbach R., Schultz M., Stefani F., 2018, *Physics reports*, 741, 1
- Shalybkov D. A., Rüdiger G., Schultz M., 2002, *Astronomy & Astrophysics*, 395, 339
- Tan X., Komacek T. D., 2019, *The Astrophysical Journal*, 886, 26